RETINAL DEGENERATION IN A KLOTHO-OVEREXPRESSING MOUSE

By

Brittany Celeste Lee

Thesis

Submitted to the Faculty of the

Graduate School of Vanderbilt University

in partial fulfillment of the requirements

for the degree of

MASTER OF SCIENCE

in

Biomedical Engineering

August, 2006

Nashville, Tennessee

Approved:

Professor Frederick R. Haselton

Professor Patricia K. Russ

ACKNOWLEDGEMENTS

I would like to thank the many people who have been instrumental in the completion of this work. I am especially grateful to Dr. Patricia Russ for her endless encouragement, expertise, and dedication to the project. I would like to thank Sai Han Presley for her patience in teaching me laboratory skills and Dr. Min Chang for giving me a home in his lab. I would also like to thank Dr. Rick Haselton for pushing me to succeed and my fellow lab mates who made the workday more pleasant. I would also like to thank my family for being ever supportive and always believing in me.

TABLE OF CONTENTS

Appendix

LIST OF TABLES

LIST OF FIGURES

CHAPTER I

INTRODUCTION

Retina

The retina, often referred to as an extension of the brain, is an integral part of the perception of sight. It is located in the posterior portion of the eye and consists of 10 layers. The ganglion cell layer is located adjacent to the vitreous. The inner limiting membrane separates these two layers. Posterior to the ganglion cells lays the inner plexiform layer, inner nuclear layer, outer plexiform layer, outer nuclear layer, photoreceptors, and retinal pigment epithelium (RPE). The inner nuclear layer is composed of horizontal, bipolar, and amacrine cell nuclei. Horizontal cells lie on the outer margin of the inner nuclear layer. Bipolar cells can be found in the middle of this layer, and amacrine cells are located on its proximal border abutting the ganglion cells. The axons of bipolar and amacrine cells make up the inner plexiform layer. The cell bodies of photoreceptors comprise the outer nuclear layer, and their axons make up the outer plexiform layer. Bipolar and horizontal cells also extend their processes into the outer plexiform layer. The external limiting membrane separates the outer nuclear layer from the photoreceptors, and the RPE, located in the back of the eye, regulates the flow of molecules between the circulation of the choroid and the neural retina [1] (Figure 1).

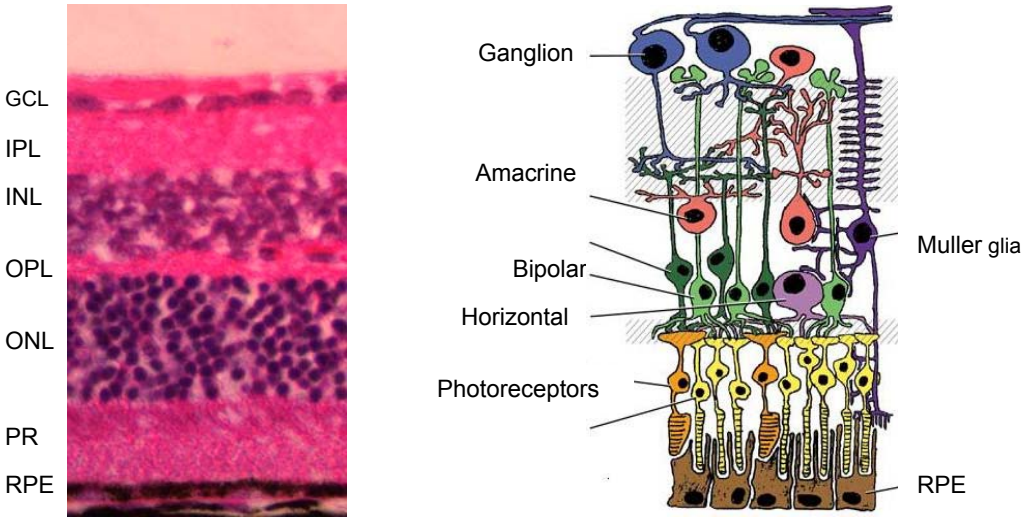

Figure 1. Histological and schematic [2] representations of the retina

When light enters the eye, it passes through the various layers of the retina to reach the photoreceptors where the visual transduction cascade is initiated. Information is relayed back through the outer layers of the retina to bipolar cells. Bipolar cells then transmit the signal to the ganglion cells, which then send the information to the brain via the optic nerve. Horizontal and amacrince cells serve to regulate the neural signal. Horizontal cells provide negative feedback for the photoreceptors to regulate the degree of excitation of the bipolar cells. Amacrine cells provide negative feedback for local signals at the inner nuclear level. These cells collect signals from multiple bipolar cells and regulate the flow of information relayed from the bipolar cells to the ganglion cells [1].

Insulin signaling, receptors, and substrates

Insulin, the most potent anabolic hormone known to date, promotes the synthesis and storage of carbohydrates, lipids, and proteins and inhibits their degradation and release into the body's circulation. The mechanisms of insulin action are complex. Consumption of food produces a rise in glucose levels, which triggers the release of insulin from the β cells of the pancreas. Insulin increases the uptake and use of glucose by skeletal muscle and fat cells by stimulating the translocation of the glucose transporter GLUT4 from intracellular sites to the cell surface [3]. The hormone also suppresses lipolysis in adipose tissue, and glucose production and ketogenesis by liver [4].

Insulin receptors are present in almost all vertebrate tissues. Embedded in the plasma membrane of cells, the receptors consist of two α subunits linked to two β subunits and each other by disulfide bonds. α subunits are extracellular and contain the insulin binding sites, and β subunits are intracellular and contain the insulin-regulated tyrosine protein kinase (Figure 2). Insulin binds to the α subunits and causes a conformational change of the dimer. This activates tyrosine kinases, which cause the autophosphorylation of tyrosine residues on the intracellular β subunits. Tyrosine kinase activity is crucial for insulin action. Naturally occurring mutations of insulin receptors that inhibit kinase activity are associated with severe insulin resistance. Once the β domains have been autophosphorylated, they can then catalyze the phosphorylation of cellular proteins such as insulin receptor substrates (IRS) 1 and 2. IRS proteins then interact with signaling molecules and cause the activation of PI3 kinase and other

cascades. The receptor structure and signaling mechanisms are similar for insulin-like growth factor (IGF) 1 [6].

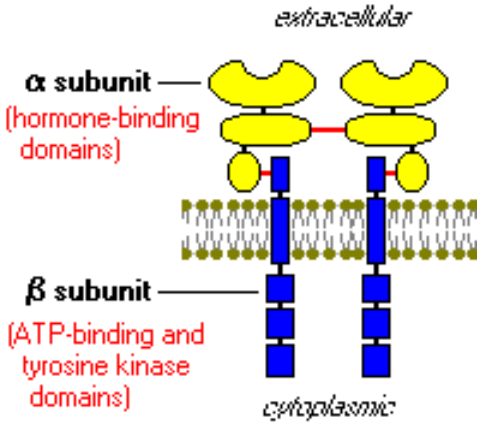

Figure 2. Insulin receptor [5]

Correct functioning of insulin signaling pathways is important for maintaining healthy blood glucose levels. It also helps prevent the retinopathy, nephropathy, neuropathy, and vascular changes associated with hyperglycemia. However, insulin resistance has also been documented to extend lifespan in animals such as *C. elegans, Drosophila*, and mice [7-9].

Insulin and the retina

Insulin receptors have been shown to be expressed in all layers of human, bovine, and rodent retinas [10, 11]. This includes neural as well as endothelial and RPE cells. Endothelial cell and pericytes have specific binding affinity for insulin, and insulin receptors on the basolateral surface of RPE cells may have a

role in one-way insulin transport to photoreceptors. Due to the relatively constant levels of insulin in the brain despite fluctuating levels in peripheral circulation, some scientists hypothesize that the insulin signaling pathway in the retina is always active and does not change with nutritional state. They further conjecture that this constant signal is required for proper development of the retina and continued cell survival [10].

Diabetes

Diabetes mellitus is characterized by deficient insulin action [10], and is projected to affect over 221 million people worldwide by 2010 [12].The disease results from the body's lack of insulin or failure to compensate for diminished insulin response and is usually characterized by high levels of circulating glucose. Type I or insulin dependent diabetes is an autoimmune disorder in which the β cells of the pancreas fail to produce insulin. It is often hereditary and accounts for about 10% of patients. Type II or noninsulin dependent diabetes comprises the majority of cases and is frequently seen in obese individuals [6]. These sufferers have become resistant to insulin or are not producing enough of the hormone to meet their metabolic needs. The Greek physician, Aretaeus, first used the term *diabetes* in the 2nd century A.D. It means "to siphon" and refers to how the disease can rapidly drain fluid from a person's body. *Mellitus* was added in the late 1700's by William Cullen. This adjective means "honey" and describes the sweetness of the blood and urine of diabetics. Until the 1900's, no reliable treatment existed for this condition. However, canine research conducted in the

early part of the century allowed scientists to create the first insulin extract, which then could be administered to prolong the life of the animals. Further progress came rapidly and by 1978, human insulin had been synthesized [13].

Diabetic Retinopathy

Diabetic retinopathy is one of the most common complications of diabetes and was first described by Jaeger in 1855 [13]. This ocular manifestation of diabetes mellitus has both vascular and neural components. Microaneurysms and dot hemorrhages are common early vascular changes. Microaneurysms are sac-like outpouchings from the sides of cellular capillaries. They have distinct margins and appear as round red spots in ophthalmologic exams. They can become completely acellular and are thought to be a secondary reaction to retinal hypoxia [4]. Hemorrhages are round red spots with indistinct borders and may appear globular or feathered depending on their location in the retina. Exudates are another clinical sign of diabetic retinopathy. Hard exudates are characterized as small, pale yellow lesions with distinct borders. These lipid-filled masses are found in the body of the retina and usually appear in areas with leaking capillaries. Soft exudates are pale yellow lesions on the surface of the retina. Often called cotton wool spots, they are indicative of neural infarcts and not really exudates at all [4]. Neuronal degeneration of all cell types in the retina has also been observed [14-19].

Klotho

Klotho was first discovered when Kuro-o and his colleagues attempted to insert a sodium–proton exchanger into C3HxC57BL/6F1 mice. Mice homozygous for the insertional transgene exhibited several phenotypes resembling human aging such as arteriosclerosis, osteoporosis, skin atrophy, ectopic calcification of certain soft tissues, a shortened life span, and infertility. Subsequent studies found that the insertional mutation disrupted the 5' promoter region of the klotho (kl) gene. The kl mutation does not disrupt the coding structure of the gene but severely reduces its expression[20].

Kl (-/-) mice develop normally up to three or four weeks of age and are indistinguishable from their wild type litter mates (+/+ or kl/+). At such time, they then begin to show growth retardation, become inactive and die between eight and nine weeks of age [20]. Age-related changes have been observed in many tissues of the klotho knockout mouse such as the lungs, skin, bone, and stomach, but the actual protein has been localized to only a few organs. These organs include the pituitary gland, placenta, skeletal muscle, bladder, aorta, pancreas, testis, ovary, colon, and thyroid gland. The human homologue has only been detected in the kidney, placenta, prostate, and small intestine [21]. Due to the limited number of tissues expressing klotho in the body and the manifestation of its effects on a number of organs, scientists hypothesized that the protein or some unidentified associated factors produce its effect through the circulatory system. To date, klotho appears to have a role in regulating calcium,

phosphorus, 1,25-$(OH)_2$ Vitamin D_3 [3], and glucose. The exact biological and molecular mechanisms, however, have yet to be elucidated [22].

The mouse klotho gene encodes a single-pass membrane protein of 1,014 amino acids (a.a.), which consists of a N-terminal signal sequence, a putative extracellular domain with two internal repeats (KL1 and KL2), a single membrane spanning region, and a short intracellular region (Figure 3).

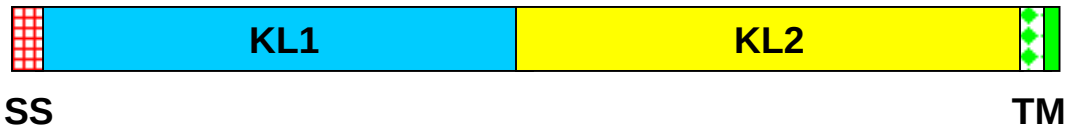

Figure 3. Structure of the klotho protein [22]

The internal repeats share homology with β-glucosidase enzymes. The human homologue of klotho is 1,012 (a.a.) in length. It has been determined that the extracellular domain is shed from the cell surface and is detectable in blood and cerebrospinal fluid of humans and mice [23]. The protein has a short stretch of basic amino acids (lys-lys-arg-lys) between the two internal repeats of the extracellular domain in both mouse and human that is a possible site for the proteolytic cleavage. A splice variant of the kl mRNA also exists which encodes for a secreted protein ~ 550 a.a. long in mice and humans. This form lacks the second internal repeat (KL2), the transmembrane domain and the intracellular domain. The secreted splice variant form of klotho has been found to predominate over the membrane form in all tissues examined in humans. The

inverse is true in wild type mice where membrane-bound klotho expression is 10 or more times greater than the splice variant [24].

Klotho has been shown to extend the lifespan of EFmKL46 and EFmKL48 mice, animals genetically engineered to overexpress the protein, through the reduction of insulin/IGF1 signaling [25]. The mechanism is believed to be the suppression of tyrosine phosphorylation of insulin/IGF1 receptors. Klotho does not affect the binding of insulin to its cell surface receptors but suppresses ligand-stimulated autophosphorylation of the receptors in a dose dependent manner. The net effect of klotho overproduction is reduced IRS activity and reduced association with PI-3 kinase [25]. Male EFmKL46 and EFmKL48 mice outlive wild type mice by 20.0% and 30.8% respectively and 18.8% and 19.0% respectively in females [25]. Male klothos are hyperinsulinemic and insulin resistant. Male and female mice are resistant to the hypoglycemic action of IGF-1 [26], have reduced GLUT4 translocation to the plasma membrane [27], and are not hyperglycemic. Thus, klotho blocks insulin signaling in a manner similar to the loss of insulin signaling seen in insulin resistance [27].

Specific aims

To date, no published works exist that document the effects altered insulin signaling induced by klotho overexpression have on the murine eye. The majority of research has focused on the anti-aging effects of klotho and it's ability to protect against cell senescence and oxidative damage [25, 28, 29]. As part of a screening study, an EFmKL46 klotho-overexpressing mouse was examined in

our laboratory and was observed to have substantial retinal vasculature leakage. This leakage was similar to that seen in rodent models of diabetic retinopathy. This observation and the fact that EFmKL46 mice are insulin resistant prompted a more detailed examination of the mouse's retinal pathology and led to the subsequent development of this research project. While many rodent models of diabetic retinopathy exist, most models are both hyperglycemic and insulin dependent or resistant. The induction of both altered insulin signaling and excess glucose in animal models make it more difficult to determine the role each has in the induction of retinopathy.

The overall objective of this project was to develop and/or utilize tools and techniques to study the klotho-overexpressing mouse and the expression of the klotho protein in murine eyes and human retinal cells. My first goal was to examine and characterize the ocular pathology observed in EFmKL46 mice. This was done using imaging techniques developed in the Haselton lab for the visualization of retinal vasculature in rodents and by various other methods employed by ophthalmologists to diagnose retinal anomalies in patients. Secondly, I needed to establish that the changes observed in these animals were caused by degeneration of the retina and not a developmental defect present from birth. This was done by examining young as well as aged EFmKL46 mice along with age and sex matched controls. As the EFmKL46 mouse has been shown to have altered insulin signaling, I aimed to correlate my findings with the ocular pathology commonly seen in diabetic patients and rodent models of deficient insulin signaling. To further support the hypothesis that the insulin-

resistant, klotho-overexpressing mouse has potential as an animal model of diabetic retinopathy, antibodies to three different peptide sequences of the klotho protein were generated to examine the expression of the protein in both murine tissues and human RPE cells. Immunohistology and western blotting were employed to demonstrate the probable presence of klotho in these tissues. Dual staining of retinal whole mounts was used to detect pericytes in an attempt to further confirm the existence of vascular anomalies caused by altered insulin signaling.

CHAPTER II

RETINAL DEGENERATION IN A KLOTHO-OVEREXPRESSING MOUSE

Abstract

PURPOSE: The klotho-overexpressing mouse, EFmKL46, is an animal model of insulin resistance that is not hyperglycemic. In this study, we evaluate the retinopathy associated with altered insulin signaling in this transgenic animal.

METHODS: In four young (8-16 weeks) and 12 aged (70-80 weeks) EFmKL46 mice along with age and sex matched wild type controls, the retinal vasculature was visualized by both fluorescence angiography and fundus photography. Photoreceptor function was evaluated by electroretinography (ERG). Tissue sections from post-mortem retinas were histologically examined for retinal layer anomalies and degeneration.

RESULTS: Aged EFmKL46 mice had abnormal retinal vasculature including tortuous veins, dot hemorrhages, and microaneurysms. Both hypo- and hyperpigmentation of the retina as well as possible retinal scarring and exudates were observed. ERG analysis showed decreased a- and b-wave amplitudes. Histological examination showed a wavy photoreceptor-retinal pigment epithelium (RPE) interface and degeneration of photoreceptors. The degeneration ranged from outer segment loss to the complete deterioration of the photoreceptor layer. The outer nuclear and outer plexiform layers were also reduced, and the remaining retinal layers were disorganized. In aged EFmKL46

mice with complete photoreceptor loss, the RPE was thickened and showed areas of RPE proliferation. No retinal anomalies were observed in young EFmKL46 and young and aged wild type mice.

CONCLUSIONS: The klotho-overexpressing mouse has retinal pathologies consistent with those seen in other animal models of insulin dependent and insulin resistant diabetes. This animal model of insulin resistance without hyperglycemia is a promising tool for more detailed studies of pathologies associated with insulin signaling dysfunction.

Introduction

Diabetes mellitus produces characteristic changes in both the retinal vasculature and the neural retina. The vascular changes associated with diabetes in patients, such as breakdown of the blood retinal barrier, capillary microaneurysms, small intraretinal hemorrhages, and pericyte loss have been well documented [12, 19, 30]. Other hallmarks of the disease include basement membrane thickening, hard exudates, and/or cotton wool spots caused by the swelling of axons in the nerve fiber layer [14, 31]. As early as the 1960's, Bloodworth [32] and Wolter [33] found that the diabetic condition also causes a loss of ganglion cells and degeneration of the inner layers of the human retina. Wolter postulated that neural retina degeneration occurs early in diabetes and may be the primary pathology that gives rise to later vascular changes [33]. Since inhibition of insulin signaling has been shown to promote apoptosis in the

neural retina [34], it has been suggested that failure of insulin/insulin-like growth factor (IGF) signaling may contribute to such retinopathy [17].

Rodent models of altered insulin signaling support the observations seen in patients. Studies of streptozotocin (STZ)-induced diabetic rats and mice have shown that neurons in the diabetic retina undergo significantly more apoptosis than those in control animals [14, 15, 33, 35]. These apoptotic neurons have been found mainly in the inner layers of the retina [14, 16, 19], but have also been observed in the outer nuclear and photoreceptor layers [14, 16]. Studies conducted with transgenic mice having mutations in the insulin 2 gene [17] or insulin receptor substrate (IRS) 2 [18] have shown similar results with loss of the inner retinal layers or outer nuclear and photoreceptor layers.

The klotho-overexpressing mouse, EFmKL46, has an extended life span which is thought to be associated with perturbations in insulin and IGF-1 signaling [25, 27]. Male klothos are hyperinsulinemic and insulin resistant. Both sexes are resistant to the hypoglycemic action of IGF-1 [26], have reduced GLUT4 translocation to the plasma membrane [27], and are not hyperglycemic. The klotho (kl) gene encodes a single pass membrane protein of 1014 amino acids with an extracellular domain composed of two internal repeats with homology to β-glucosidases [24]. The extracellular domain of klotho is cleaved and secreted into the blood. This fragment then binds to the cell surface and blocks or inhibits insulin signaling by suppressing tyrosine phosphorylation of insulin/IGF-1 receptors. While the protein does not prevent insulin from binding to its ligand receptors, the net effect is reduced IRS activity and reduced

association with PI-3 kinase. Thus, klotho blocks insulin signaling in a manner similar to the loss of insulin signaling seen in insulin resistance [27].

While many rodent models of diabetic retinopathy exist, most models are both hyperglycemic and insulin dependent or resistant. The induction of both altered insulin signaling and excess glucose in animal models makes it more difficult to determine the role each has in the induction of retinopathy. In this paper, we characterize the ocular pathology present in the nonhyperglycemic, insulin resistant EFmKL46 mouse.

Methods and materials

Animals

EFmKL46 and wild type mice were obtained from the University of Texas Southwestern Medical Center at Dallas [20]. The Institutional Animal Care and Use Committee at Vanderbilt University approved all animal experiments, and animals were treated in accordance with the ARVO Resolution on the Use of Animals in Research and Institutional Guidelines. Mice weighing 20-50g were anesthetized with an intraperitoneal injection of ketamine/xylazine (87mg/kg/13 mg/kg). Both eyes were dilated with one drop each of tropicamide (1%) and phenylephrine (2.5%) and covered with methylcellulose (2.5%) to prevent drying of ocular media. Fluorescence angiography, fundus photography, or ERG was then performed. Animals were euthanized by cervical dislocation, and the eyes were removed for sectioning. Paraffin sections were hematoxylin and eosin (H & E) stained to view histology.

Fluorescence angiography

Angiography was performed as previously described [36]. Briefly, animals were anesthetized and their eyes dilated as described above. Mice were placed on the stage of an inverted fluorescence microscope (Nikon Eclipse TE2000-U, Nikon, Inc., USA) with the eye placed in a –6 diopter lens containing 2.5% methylcellulose to reduce light refraction. The microscope apparatus included a 120 watt light source (EXFO X-Cite 120 Fluorescence Illumination System, EXFO, Ontario, Canada), a filter cube for excitation and emission of fluorescein, and a 4X objective (Figure 4). Each animal received a 50μL injection of sodium fluorescein (25mg/ml) intraperitoneally. Immediately after injection, retinal vessels of both eyes were imaged with a 3CCD digital camera (Hamamatsu C7780, Hamamatsu Photonics K.K., Hamamatsu City, Japan) and Image Pro software.

Fundus photography

After the mouse was anesthetized and its pupils dilated as described above, it was placed on an examination table and positioned below the lens of a Zeiss surgical microscope (OPMI 1-FC, Carl Zeiss, Inc., West Germany). A 90 diopter lens was placed between the animal and the microscope and adjusted until the image of the retina was focused in the eyepiece. A digital camera (Nikon D100, Nikon, Inc., USA) mounted to the surgical microscope was utilized to capture fundus images.

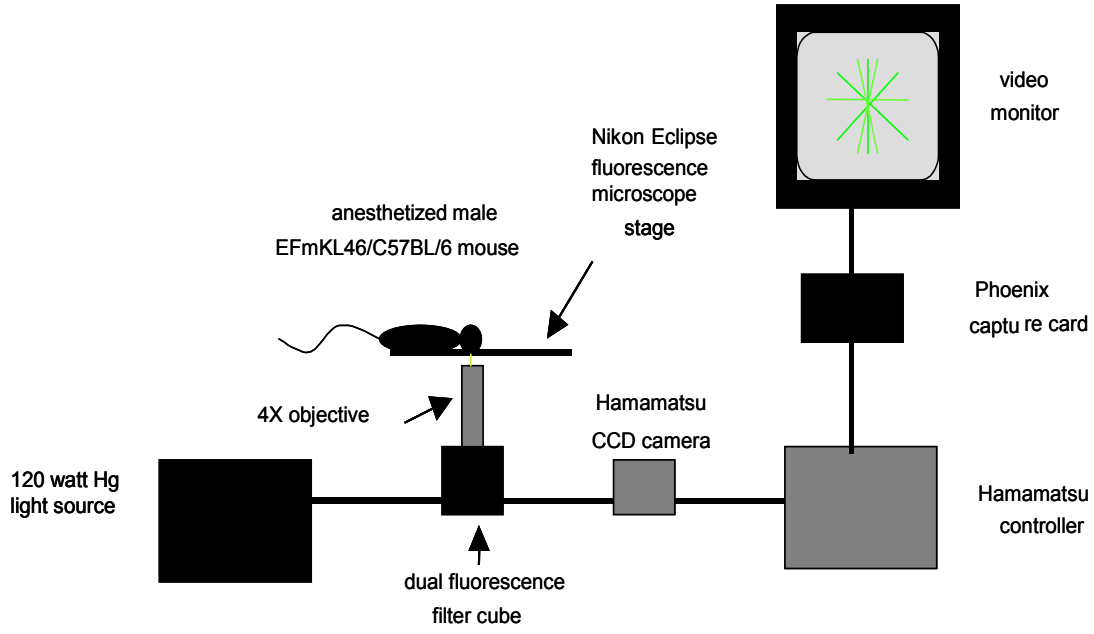

Figure 4. Diagram of fluorescence microscope configuration

Electroretinography

Following an overnight dark-adaptation period, electroretinograms were performed as previously described [37]. Briefly, animals were anesthetized and their eyes dilated as described above. A DTL silver/nylon fiber recording electrode (Diagnosys LLC, Littleton, MA) was placed on the corneal surface of each eye and held in place by a drop of methylcellulose. Needle electrodes placed subcutaneously in the forehead and tail served as reference and ground leads respectively. Mice were placed in front of a Ganzfield dome on a heated pad to ensure normal body temperature was maintained at 37°C. Rod-driven responses to light flashes covering an intensity range of 2.5-600.5 cd sec/m^2 were recorded by a visual electrodiagnostic system (UTAS-E 3000 with EM for Windows, LKC Technologies, Inc., Gaithersburg, MD). The responses were

amplified at 2500 μV and high and low pass filtered at 0.05 Hz and 500 Hz respectively.

Results

Histological studies revealed neural degeneration

Histological sections from aged EFmKL46 indicated a disorganized retinal structure (Figure 5, D-H). Pathologic findings ranged from a loosely organized inner nuclear layer and patchy photoreceptors to the complete absence of outer plexiform, nuclear, and photoreceptor layers. Mild pathology was observed as a wavy RPE-photoreceptor interface, shortened outer segments, and patchy loss of inner segments of the photoreceptor layer (Fig. 5, D). The outer segments in two klotho mice were observed to be partly degenerated or absent (Fig. 5, E). The complete loss of photoreceptors as well as the outer nuclear and plexiform layers was seen in two thirds of the mice examined (Fig. 5, F-H). Hypertrophy of the RPE layer was observed in aged EFmKL46 mice, extending as far into the retina as the inner plexiform layer (Fig. 5, G-H). Extraneous pigmentation was present in the inner layers of the retina, including the ganglion cell layer, in three-fourths of the aged klotho animals examined (Fig. 5, G). Sections from wild type mice (Fig. 5, A, C) and young EFmKL46 mice (Fig. 5, B) were similar to that of a normal mouse retina in both the central and peripheral regions.

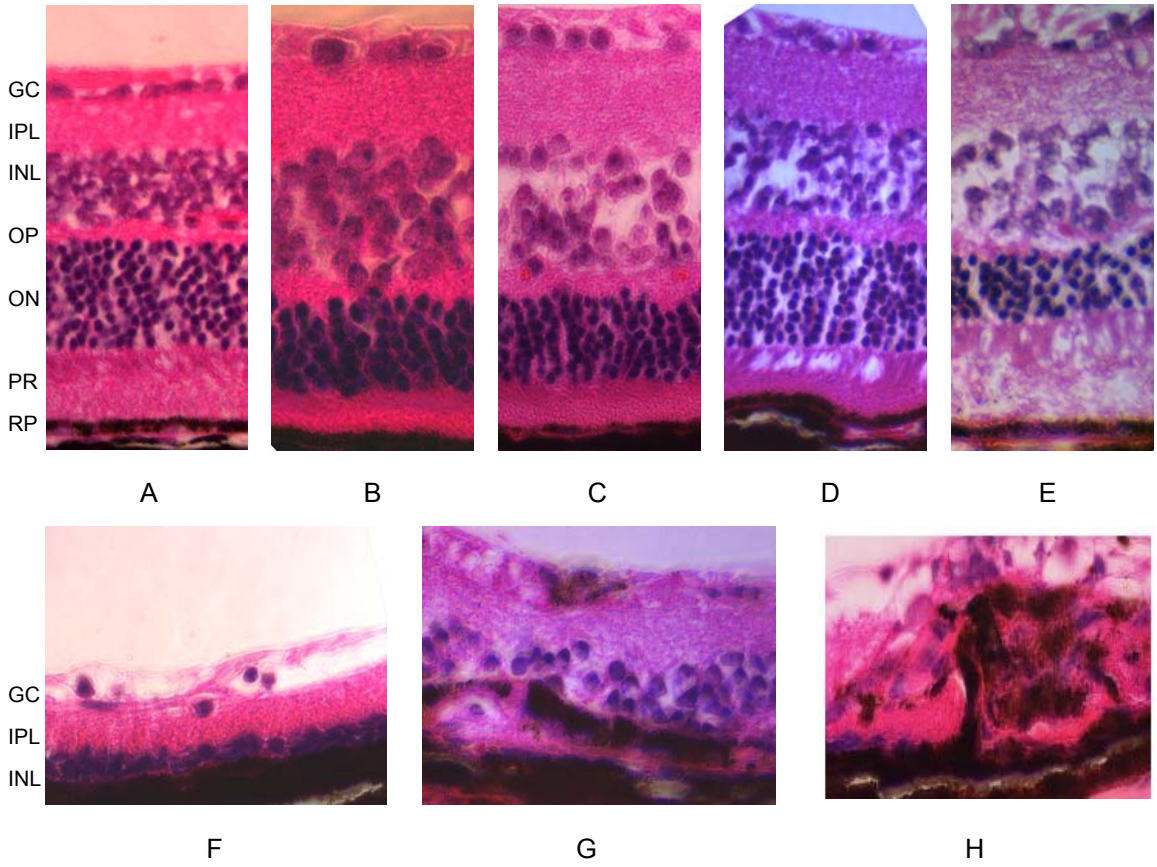

Figure 5. Retinal Histology. Sections of young wild type (A), young EFmKL46 (B), and old wild type mice (C) are similar with well organized cell layers that are easily distinguished from adjacent layers. The pathology seen in aged EFmKL46 mice progresses from the outer to inner retina. Waves at the RPE-photoreceptor interface, outer segment shortening, and holes in the inner segments were observed with little change to inner retinal layers (D). In severe photoreceptor degeneration (E), the outer plexiform layer appears to be reduced as well. The complete disappearance of the photoreceptors, outer nuclear layer, and outer plexiform layer, and loss of ganglion cells is seen as retinal thickness continues to decrease (F-H). Proliferation of the RPE into the inner layers of the retina (G-H) and brown spots in the inner plexiform/ganglion cell layer were also seen (G). GCL=ganglion cell layer; IPL=inner plexiform layer; INL=inner nuclear layer; OPL=outer plexiform layer; ONL=outer nuclear layer; PR=photoreceptors; RPE=retinal pigmented epithelium.

Fluorescence angiography showed vascular abnormalities

Aged EFmKL46 mice exhibited several types of vascular pathologies including tiny hemorrhages in the microcirculation (Figure 6, C-D) and early retinal branch vein occlusions (Fig. 6, D, F). Fluorescein leakage in the peripheral retina, neovascular tufting and microaneurysms were also observed

(Fig. 6, E-F). Fluorescein angiography performed on age and sex matched wild type (data not shown) and young EFmKL46 (Fig. 6, A-B) mice showed normal retinal vasculature.

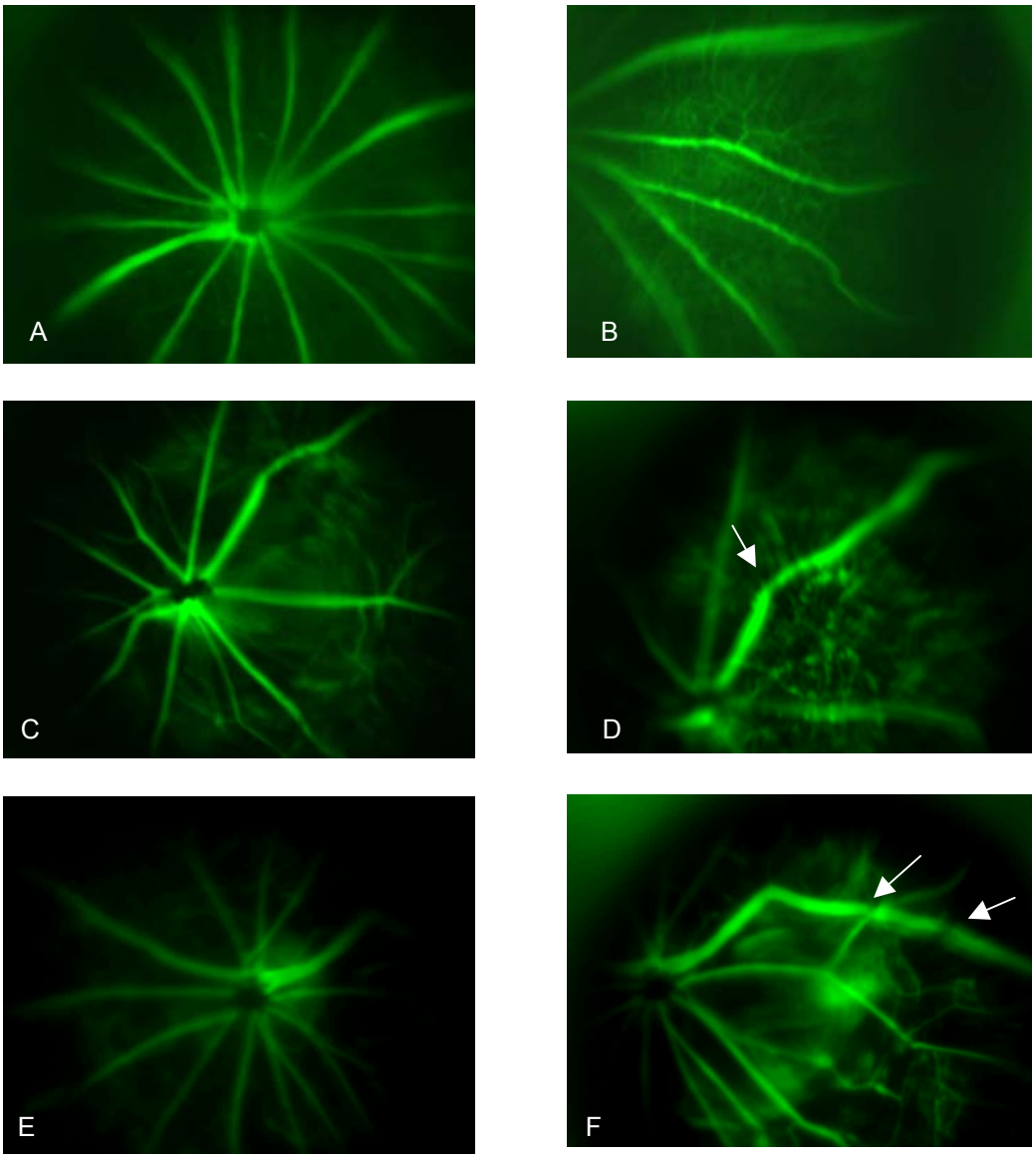

Figure 6. Fluorescence angiography. The optic nerve head (A,C,E) and the peripheral retina (B,D,F) of both wild type/young EFmKL46 (A-B) and aged EFmKL46 mice (C-F) show very different vasculatures. The wild type mice have normal vessels and the microcirculation can clearly be seen in the peripheral photograph. Aged EFmKL46 show vascular anomalies (C-F). Abnormal central vascularutre (C) as well as small hemorrhages in the microcirculation and early retinal vein occlusions (D, F arrows) were observed. Leakage of the retina vessels as well as neovascularization and tufting also can be seen (E-F).

Fundus photography indicated retina damage

In aged EFmKL46 mice (Figure 7, B-D), areas of hypo- and hyperpigmentation were observed in the periphery. Small, yellow spots were also present as well as areas of possible scarring (Fig. 7, C), non-profused and/or tortuous vessels, and abnormal color variation near the optic disk (Fig. 7, B). A distinct line of demarcation existed between the hypo- and hyperpigmented areas (Fig. 7, D). In two-thirds of the animals examined, a haziness of the lens was also observed indicating the possible formation of a cataract. In wild type (Fig. 7, A) and young klotho mice (data not shown), the fundus images appeared normal, and no defects were observed.

ERG recordings showed decreased rod response

Aged EFmKL46 mice exhibited decreased a- and b-wave responses to all flash stimuli presented as compared to control animals (Figure 8). The amplitude of aged EFMKL46 a-wave responses peaked at 300 cd sec/m^2 and then decreased. Control animal a-wave responses increased with stimulation intensity from 2.5–600 cd sec/m^2 (Fig. 8, C). B-wave amplitudes for aged EFmKL46 had a very moderate increase and peaked at 450 cd sec/m^2 while control amplitudes increased over the range of intensities examined (Fig. 8, D).

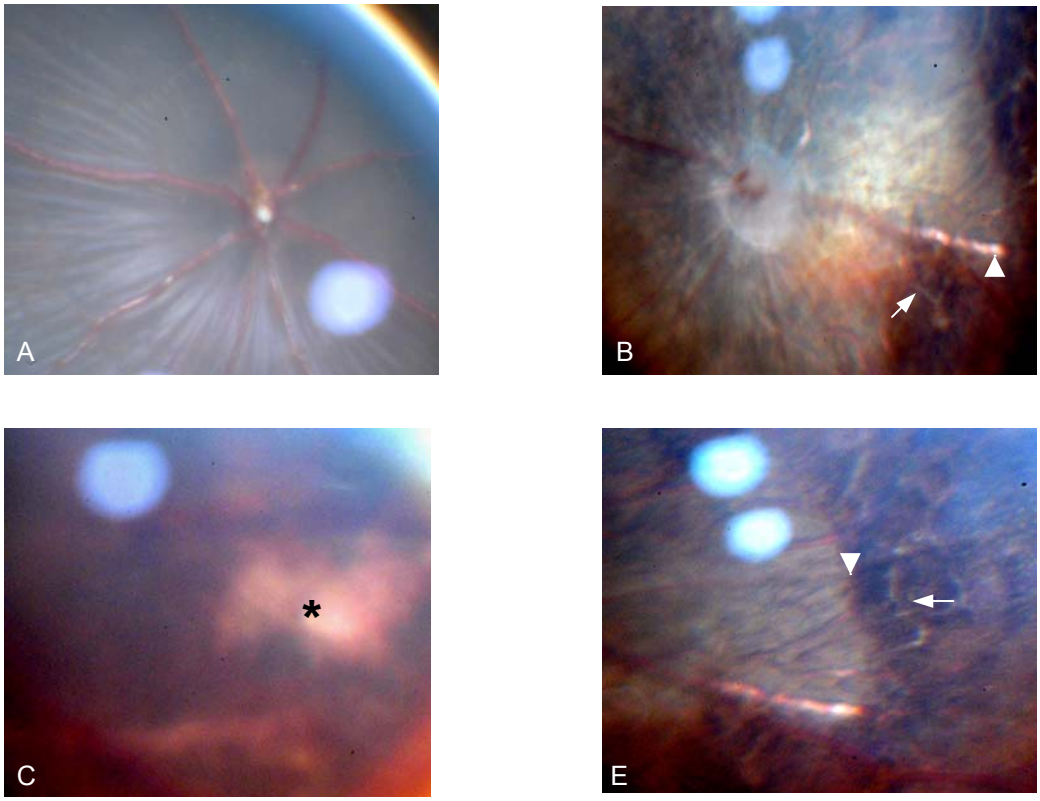

Figure 7. Fundus photography. Both aged wild type and young EFmKL46 mice were observed to have normal retinas (A). Note the healthy blood vessels and striations of the neural layers. Hypo- and hyperpigmentation of peripheral retina (B, D) and areas of scarring (C*) were observed in aged EFmKL46 mice. Yellowish spots and brown pigmentation (B*) can be seen as well as tortuous vessels of the microcirculation (B, arrow) and a nonprofused vessel (B, ▲). Also note the paleness of the optic disc. A more peripheral view of B (D) shows the sharp contrast between the hypo- and hyperpigmented areas (D, ▼) as well as the vessels in the microcrculation (D, arrow). The hypopigmented area has the shape of a four-leaf clover.

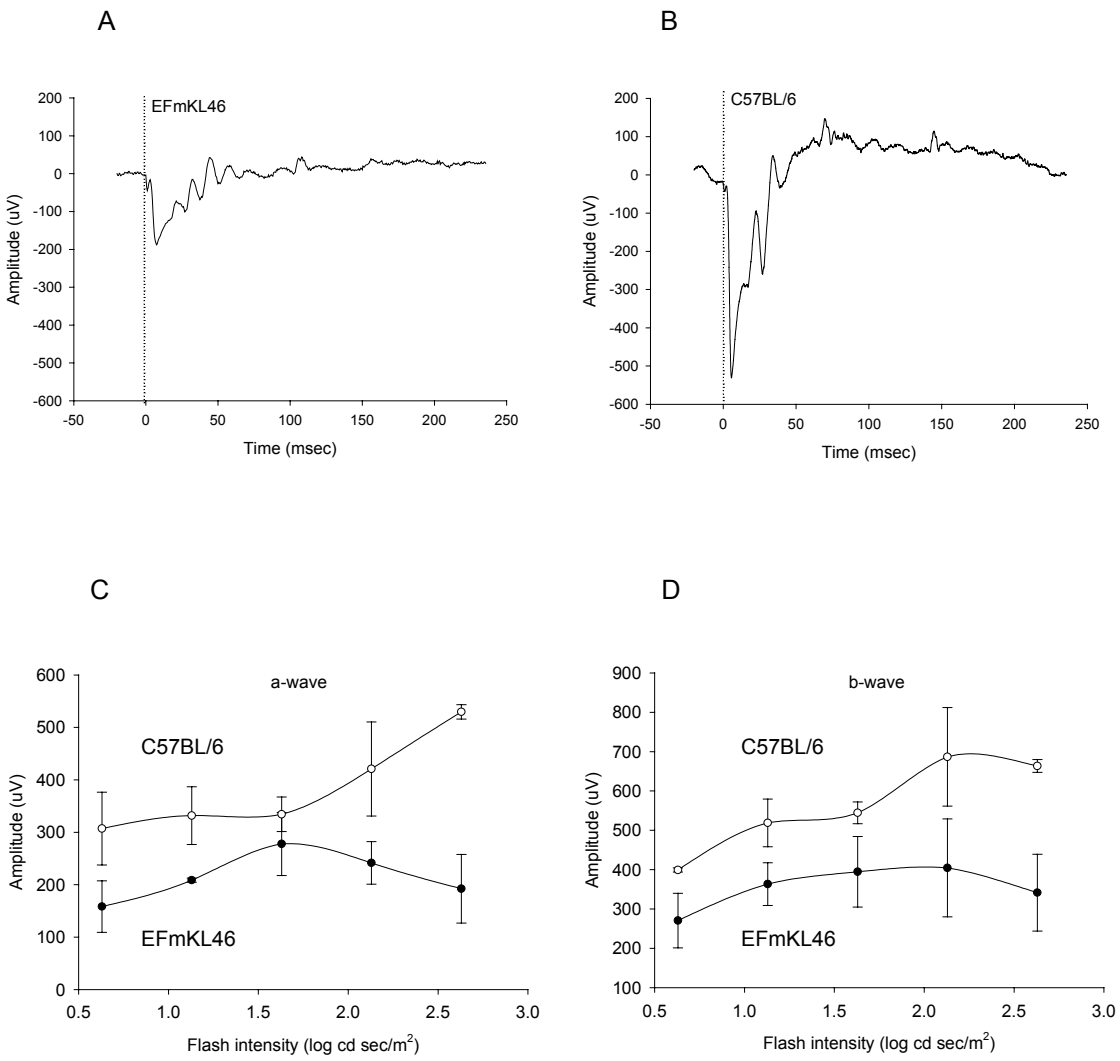

Figure 8. ERG data. Representative ERG signals recorded on the corneal surfaces of aged EFmKL46 and control animals at 600.5 cd sec/m^2 (A-B). Both the a- and b-waves of the ERG waveforms show severely decreased response to light stimuli in aged EFmKL46 mice as compared to control animals (C-D). This effect can be seen more clearly at flash intensities greater than 2 log cd sec/m^2.

Discussion

Aged EFmKL46 mice exhibit degeneration of the neural retina most prominently in the outer plexiform, nuclear, and photoreceptor layers. This is shown in histological sections (Figure 5) and supported by ERG data (Figure 8).

This result is consistent with the hypothesis that dysfunctional insulin signaling in the retina contributes to neural retina cell death, recently reviewed in Reiter and Gardner [10]. To date, one of the difficulties in obtaining experimental data in support of this hypothesis has been the development of a suitable animal model, as hyperglycemia is usually induced with the disruption of insulin signaling. Aged EFmKL46 animals are insulin resistant, not hyperglycemic, and yet they characteristically show a loss of photoreceptors.

Our findings correlate most closely with published studies on the $IRS2^{-/-}$ mouse model of insulin resistance. IRS 1 and 2 mediate many functions of insulin and IGF through the PI-3 kinase - Akt cascade [18], and insulin and IRS activity in the aged klotho mouse is severely decreased. Yi et al found that the IRS 2 receptor was located in the outer and inner plexiform layers, ganglion cells, and inner photoreceptor segments, and $IRS2^{-/-}$ mice exhibited a loss of photoreceptors followed by uniform thinning of the outer nuclear layer [18].

$IRS2^{-/-}$ mice normally die from extreme hyperglycemia, but β cell function was restored by transgenic expression in β cells of the nuclear transcription factor Pdx1 ($IRS2^{-/-}$::$Pdx1^{tg}$). These mice are insulin resistant but do not develop diabetes. Results from partially rescued $IRS2^{-/-}$::$Pdx1^{tg}$ animals closely match our findings and support the hypothesis that dysfunction of the insulin/IGF signaling cascade, rather than hyperglycemia, induces photoreceptor loss. These animals displayed a progressive loss of photoreceptors, reduction of the outer nuclear layer, and moderate loss of inner retinal layers with all retinal layer loss occurring after photoreceptor degeneration. In the same study, $IRS1^{-/-}$ mice that developed

glucose intolerance but not diabetes showed no changes in the retina [18]. Yi et al proposed that the IRS 2 receptor promotes photoreceptor survival by inhibiting the caspase activation cascade, as activated caspase 3 correlates with photoreceptor degeneration in several rodent models and accumulates in the retina of IRS2 $^{-/-}$ mice. Determining caspase 3 levels in aged klotho mice has not been done but would provide additional biochemical data to evaluate this hypothesis.

Several other published reports suggest that insulin resistance, apart from hyperglycemia, causes neural retina degeneration. Insulin reduces neuronal cell death in cerebral ischemia independent of blood glucose levels [38]. In addition, antibodies that inhibit insulin signaling have been shown to promote apoptosis of the neural retina [34].

Other models of the diabetic state have shown some of the pathology we observed in aged klotho mice. For example, loss of the blood retinal barrier and reduction of the inner layers of the retina was documented in hyperglycemic mice with a point mutation of the insulin 2 gene [17]. In one study of STZ-treated rats, a slight thinning of the inner retina, a gross reduction in outer nuclear layer thickness, and the death of photoreceptors were shown as the duration of insulin-dependence increased [14]. Others found a degeneration of the inner plexiform layer as well as the photoreceptor and RPE layers in STZ rats [16], or reported loss of inner nuclear and plexiform layers with ganglion cell loss [19]. Mice made insulin dependent with STZ were found to have loss of ganglion cells and inner and outer nuclear layers [15].

After the photoreceptors and outer nuclear and plexiform layers of aged EFmKL46 mice are lost, RPE infiltration and proliferation into the inner layers of the retina was observed (Figure 5, F-H). These changes could be attributed to deterioration of the blood retinal barrier as fluorescein leakage was seen during angiography testing (Figure 6, C-F). To maintain proper homeostasis of the retina, the RPE must preserve its integrity and protect the neural layers from the open circulation of the choroid. When the blood retinal barrier is disrupted, growth factors, proteins, and other molecules can pass unregulated between the two environments. While the klotho protein is highly specific for insulin/IGF-1, it does not affect the binding or activity of other growth factors such as epidermal growth factor (EGF) and platelet-derived growth factor (PDGF) [25]. PDGF has been found to be one of the main chemoattractants for RPE cells, and EGF can stimulate proliferation of epidermal and epithelial cells. The response to EGF is enhanced under hypoxic conditions in which the number of receptors per cell increases [39], and patients suffering from diabetes have increased EGF and PDGF levels [40].

Abnormalities of the fundus and decreased a- and b-wave amplitudes were only observed in aged klotho mice. Vascular anomalies detected with angiography and fundus photography were seen only in aged EFmKL46 mice with degenerated outer retinal layers. These findings correlate well with reports that have found retinal degeneration occurs in the neural retina before vascular changes become apparent [12, 14, 15, 19]. The severity of retinal histological changes correlates closely with the degree of vascular and pigmentation

anomalies and decreased neural signaling observed with the diagnostic techniques used in this study. As with patients, the retinal pathologies seen in aged EFmKL46 mice vary among animals. Future studies are needed to further elucidate the reason(s) for animal-to-animal variation.

Microaneurysms, diffuse leakage, dot hemorrhages, and tortuous veins were observed with fluorescence angiography and fundus photography in aged klotho mice. These vascular changes are among the main complications of diabetic retinopathy and are thought to be the result of metabolic damage to vascular endothelial cells [30]. Although hyperglycemia is most often the strongest predictor of diabetic complications, several well-documented cases of diabetic retinopathy have been described in patients without overt hyperglycemia or glucose intolerance [10]. These cases suggest that insulin resistance may be required for the development or progression of retinopathy.

The retinal pathologies observed in aged EFmKL46 mice appear to be the result of a progressive degeneration, not a developmental defect. As can be seen in Figure 5, young EFmKL46 mice have retinas similar to young and old wild type mice with complete development of all retinal layers. Fluorescence angiography and fundus photography in Figures 6 and 7 show no observable vascular anomalies in young klothos.

Previous studies on the EFmKL46 mouse have explored the biochemical basis for their increased longevity. Kuro-o et al recently published data suggesting that klotho-induced insulin resistance increases their lifespan [25]. Kuro-o et al have demonstrated that the klotho protein in the EFmKL46 mice

binds to cell surface receptors and results in resistance to insulin and IGF-1. Its mechanism is believed to be the suppression of tyrosine phosphorylation of insulin/IGF-1 receptors, which leads to the reduction of IRS activity and association with PI-3 kinase. This mechanism has been hypothesized to be beneficial for peripheral tissue by preventing cellular lipid overload via reduction of the insulin-stimulated availability of glucose. A reduced intracellular lipid content could raise the apoptotic threshold and extend the life of cells [27]. However, our data suggests that the altered signaling appears to result in the loss of photoreceptors and further retinal degeneration.

In summary, the retinal pathology exhibited by the aged EFmKL46 mouse has characteristics similar to those seen in patients with diabetes and rodent models of altered insulin signaling. The principle observation is loss of photoreceptors, which occurs in all aged klotho mice. More severe pathology such as vascular leakage and RPE proliferation is variable among animals. Based on comparisons with published studies, our results are consistent with the hypothesis that dysfunction of the insulin/IGF-1 signaling cascade, rather than hyperglycemia, is responsible for neuronal cell death in the retina. The klotho-overexpressing mouse is a promising animal model for further detailed studies of retinal pathologies associated with altered insulin signaling and may prove useful for specifically studying the role insulin and IGF-1 in retinal function and maintenance.

CHAPTER III

SUMMARY AND FUTURE WORK

In summary, the retinal pathology exhibited by the aged EFmKL46 mouse has characteristics similar to those seen in patients with diabetes and rodent models of altered insulin signaling. The principle observation is loss of photoreceptors, which occurs in all aged klotho mice. More severe pathology such as vascular leakage and RPE proliferation is variable among animals. Based on comparisons with published studies, these results are consistent with the hypothesis that dysfunction of the insulin/IGF-1 signaling cascade, rather than hyperglycemia, is responsible for neuronal cell death in the retina.

Future studies on the EFmKL46 mouse would contribute to a better understanding of the animal and the biological cause(s) of its retinal pathology. The effects altered insulin signaling has on the eyes of female EFmKL46 mice have not been examined. These animals are resistant to IGF-1 but not insulin. While insulin and IGF-1 are believed to have similar mechanisms of action, they are not identical. Since the longevity of EFmKL46 females may be induced without altering insulin levels or actions [26], these mice could exhibit different ocular pathologies. If this is shown to be the case, a comparison between the sexes would be of use. The changes seen in males versus females could be categorized and then compared to hypothesize how the resistance to each

hormone contributes to ocular pathology. This could help determine the role IGF-1, as opposed to insulin, has on the degeneration of the retina.

EFmKL48 mice have also been found to be insulin and IGF-1 resistant. These animals overexpress the klotho protein, but the transgene has been inserted in a different, unknown location in the genome. Due to access limitations at the time of this project, no experimentation could be performed on these animals. Conducting the same type of experiments with EFmKL48 mice and comparing results to EFmKL46 could bring to light possible difference between the two strains. Observing the same ocular pathologies in both strains would also help to confirm that the changes observed in EFmKL46 mice are, in fact, due to insulin/IGF-1 resistance and not the disruption of an unknown gene by the insertion of the klotho transgene.

Samples from the vitreous of klotho-overexpressing mice could also be obtained to determine the levels of glucose, insulin, and growth hormones such as EDF, PDEGF, VEGF, and then compared to controls animals. These growth hormones have been found to induce the proliferation and migration of RPE cells in vitro and are present in diabetic patients' plasma and serum at higher concentrations than in nondiabetic patients. These growth factor levels could be measured to determine if the growth factor levels are also increased in the insulin-resistant EFmKL46 mouse as compared to wild type mice.

Preliminary work with three polyclonal antibodies for the klotho protein has also been performed and is documented in Appendix A. This work indicates that both the membrane and splice variant forms of the klotho protein are potentially

present in both the retinas of EFmKL46 and control C57BL/6 mice, and human RPE cells. Future work should be focused on confirming the specificity of these antibodies. This could be done by repeating the experiments detailed in Appendix A with the monoclonal antibodies KM2076 and KM2119 [21]. These have been proven to recognize the membrane and splice variant forms in humans and mice in western blot and immunofluorescent applications. Also, additional western blots should be performed with our antibodies to confirm the preliminary results presented in Appendix A. Immunohistochemistry should also be done with wild type mouse kidneys [20, 21, 41], and human kidney and eye tissue to further substantiate our antibodies' validity. While these antibodies may not prove useful for western blotting, they may still have utility for immunohistochemistry.

Confirming the specificity of our antibodies will then enable them to be used for a variety of experiments such as discovering expression of the klotho protein in the retinas of humans, determining its location in the mouse retina, and differentiating which form of the protein is present. This work could also lead to further studies on the interaction of klotho with insulin receptors in the eye. Cellular experiments could also be conducted to elucidate the effect increased or decreased klotho expression has on cells such as the RPE. Oxidative stress testing, for example, could be conducted to determine if cell senescence is reduced in RPE cells that overexpress the protein.

Pericyte loss has also been preliminarily examined and is documented in Appendix C. These results are inconclusive. Neither the presence nor loss of

pericytes could be definitively confirmed. Future work should refine the staining procedure employed or a standard trypsin digest of the retina should be used to determine if EFmKL46 mice have pericyte loss. As pericyte dropout is one of the hallmarks of diabetic retinopathy, this finding could clarify whether this cell type is being lost in the insulin resistant EFmKL46 mouse or if other mechanisms should be explored to explain the pathology.

APPENDIX A

KLOTHO ANTIBODIES AND IMMUNOSTAINIG

Introduction

Klotho has been shown to extend the lifespan of EFmKL46 and EFmKL48 mice, animals genetically engineered to overexpress the protein, through the reduction of insulin/IGF1 signaling [25, 27]. The mouse klotho gene encodes for a single-pass membrane protein of 1,014 amino acids (a.a), which consists of an N-terminal signal sequence, a putative extracellular domain with two internal repeats (KL1 and KL2), a single membrane spanning region, and a short intracellular region (Figure 9).

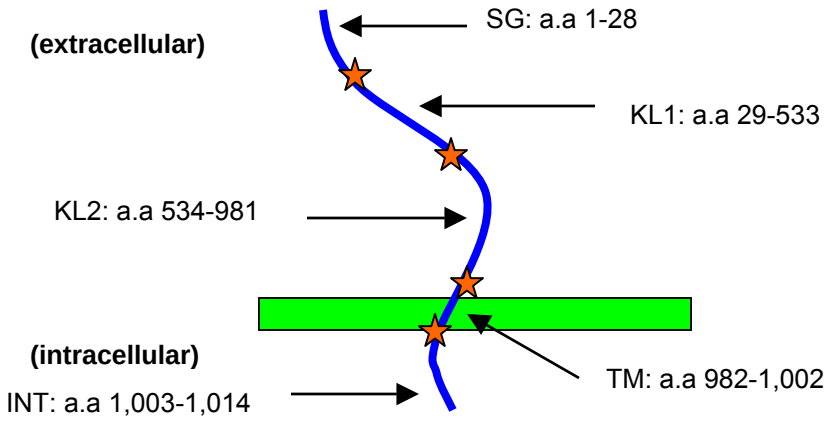

Figure 9. Mouse klotho membrane protein structure. SG= signaling sequence, KL1= first klotho repeat, KL2= second klotho repeat, TM=transmembrane regionn, INT= intracellular region, a.a.=amino acid.

The internal repeats share homology with β-glucosidase enzymes. The human homologue of klotho has 86% amino acid identify to the mouse klotho protein and is 1,012 a.a. in length [22]. The protein has been detected in the pituitary gland, placenta, skeletal muscle, bladder, aorta, pancreas, testis, ovary, colon, and thyroid gland of mice and the kidney, placenta, prostate, and small intestine in humans [21]. Due to the limited expression of klotho in the body but the manifestation of its effects on a number of organs, scientists hypothesize that the protein or some unidentified associated factors produce its effect through the circulatory system. It has been determined that the extracellular domain of klotho is shed from the cell surface and is detectable in blood and cerebrospinal fluid of humans and mice [23]. The protein has a short stretch of basic amino acids (lys-lys-arg-lys) between the two internal repeats of the extracellular domain in both mouse and human that is a possible site for the proteolytic cleavage. A splice

variant of the kl mRNA also exists which encodes for a secreted protein ~ 550 a.a. long in mice and humans.

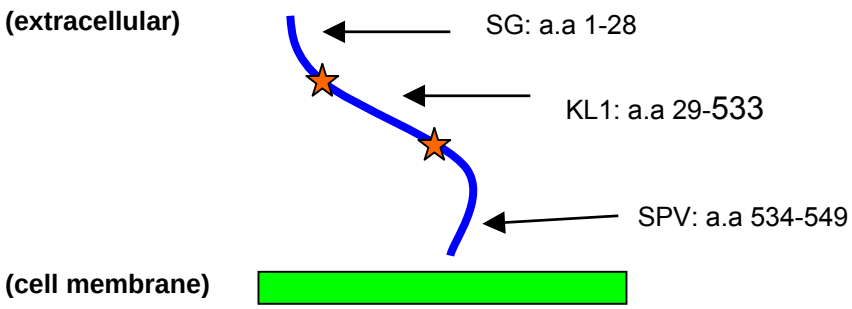

Figure 10. Mouse klotho splice variant protein structure. SG= signaling sequence, KL1= first klotho repeat, SPV= a.a. unique to splice variant.

This form lacks the second internal repeat (KL2), the transmembrane domain and the intracellular domain. The secreted splice variant form of klotho has been found to predominate over the membrane form in all tissues examined in humans. The inverse is true in wild type mice where membrane-bound klotho expression is 10 or more times greater than the splice variant [24].

Recent work has shown that the klotho protein has anti-apoptotic and anti-senescence effects on vascular endothelial cells [28]. However, studies in our lab have shown that aged EFmKL46 mice have disruption and proliferation of the retinal pigment epithelium as well as retinal degeneration hypothesized to be the result of apoptosis. In this work, we sought to explore the potential expression and distribution of the klotho protein in the mouse eye and human RPE cells.

Methods and materials

Antibodies

Polyclonal antibodies were generated to three different peptide sequences of the human klotho protein [42] (Zymed Laboratories, San Francisco, CA). KL-I ((C)YYSKKGRRSYK-$_{COOH}$) corresponded to amino acids (a.a.) 1002~1012 located in the intracellular domain; KL-S ((C)SQLTKPISSLTKPYH-$_{COOH}$) corresponded to a.a. 535~549, which were unique to the splice variant of the protein, and KL-B ((C)SGTTKRDDAKYMYY-$_{NH_2}$) corresponded to a.a. 420~433 located in the first klotho repeat (KL1) of the extracellular domain. Mice and humans share 80% homology for the protein (ref). NCBI Basic Local Alignment Search Tool (BLAST) was utilized to ensue that these a.a. sequences were homologous to other proteins found in rodents or humans. Other primary antibodies used were specific for NG2 and biotinylated lectin. Secondary antibodies used were Alexa Fluor 488, 568, and 680 conjugated goat anti-rabbit IgGs. 4,6-diamidine-2-phenylindole dihydrochloride (DAPI) nucleic acid stain was also used (Molecular Probes, Eugene, Oregon).

Cell Culture

All experiments were performed using ARPE-19, a human retinal pigment epithelium cell line (ATCC, Manassas, VA). Cells were seeded at a density of 15,000/cm^2 on 4-chamber slides, and cultures were maintained for 2 or 3 days.

on slides and 1 week in plates. DMEM medium supplemented with 10% fetal bovine serum was changed twice a week.

Immunofluorescence

Immunohistochemistry was conducted to determine the expression and/or localization of the klotho protein in ARPE-19 cells and mouse retinal tissue. Cells grown on 4-chamber slides were fixed with 70% methanol for 15 minutes, rinsed with PBS and permeabilized with 0.25% Triton X-100 for 10 minutes, and blocked with a solution of 2% BSA in 1X PBS for 1.5 hours at room temperature. Frozen tissue sections from aged EFmKL46 and C57BL/6 mice retinas were fixed and permeabilized in the same manner. Frozen sections were blocked with a solution of 5% bovine serum and 2% BSA in PBS overnight at 4°C. Primary klotho antibodies were then added at a dilution of 1:250 and incubated overnight at 4°C. After being washed three times with PBS, the secondary antibody and DAPI were added to the sample at dilutions of 1:1500 and 1:2000 respectively. After a 4-hour incubation period at room temperature, slides were washed five

All slides were examined with an inverted fluorescence microscope (Nikon Eclipse TE2000-U, Nikon, Inc., USA) with an EXFO X-Cite 120 Fluorescence Illumination System. Pictures were taken with a 3CCD Digital Camera (Hamamatsu C7780, Hamamatsu Photonics K.K., Hamamatsu City, Japan) and Image Pro software.

Western blotting

Since the kidney is one of the primary organs to express the klotho protein in mice, western blotting was conducted on kidney lysates to test the validity of the three generated antibodies. Eye lysates were used to determine if the klotho protein was present in the murine eye. Frozen eye and kidney tissues from C57BL/6 mice were homogenized in lysis buffer ([1% Triton X-100, 10%glycerol, 1% NP-40, 50 mM Hepes, pH 7.4, 100 mM sodium pyrophosphate, 100 mM sodium fluoride, 10 mM EDTA, 5 mM sodium vanadate, aprotinin (10 µg/ml), leupeptin (5 µg/ml), benzamidine (1.5 mg/ml), and PMSF (34 µg/ml]) [43] using a sonic dismembrator (Fisher Model 100, Fisher Scientific) at a speed of 2 for 10 s intervals. The insoluble material was removed by centrifugation at 14,000 rpm for 1.5 hours. 20 µg of supernatant proteins measured by BCA protein assay kit (Pierce Biotechnology, Inc., Rockford, IL) were separated on SDS-PAGE gel (10%) and transferred electrophoretically to a PVDF membrane. Blots was blocked in PBS with 0.1% Tween 20 and 2% bovine serum albumin for 1 hr at room temperature and incubated with 1 µl/ml of each primary antibody overnight at 4˚C. They were then washed and subjected to treatment with the secondary antibody at a dilution of 0.2 µl/ml for 45 minutes. Blots were washed again and then dried. Bands were visualized with the Odyssey Infrared Imaging System (LI-COR, Biotechnologies, Lincoln, NE).

Results

Western blot analysis of klotho protein

Western blot analysis produced multiple bands from both eye and kidney lysates when probed with the KL-I antibody (Figure 11, A). Dual bands of ~35 and ~ 90 kDa were detected for eye and kidney lysates. Eye lysates also showed lower bands estimated to be 22 and 33 kDa. A band between 93 and 115 kDa was also detected from kidney lysates. Bands detected from eye lysates with KL-S roughly correspond to the two lower bands from eye lysate detected with KL-I (Fig. 11, B). Their sizes were estimated to be 22 and 35 kDa. A possible band was also detected for 115 kDa. The faint bands appearing on the blot between 50 and 93 kDa are an image artifact. They are not as dark on the original scan of the blot and are believe to be the result of formatting and transferring the image. No bands were visualized from the kidney lysate using KL-S (data not shown). No bands were detected with KL-B (data not shown).

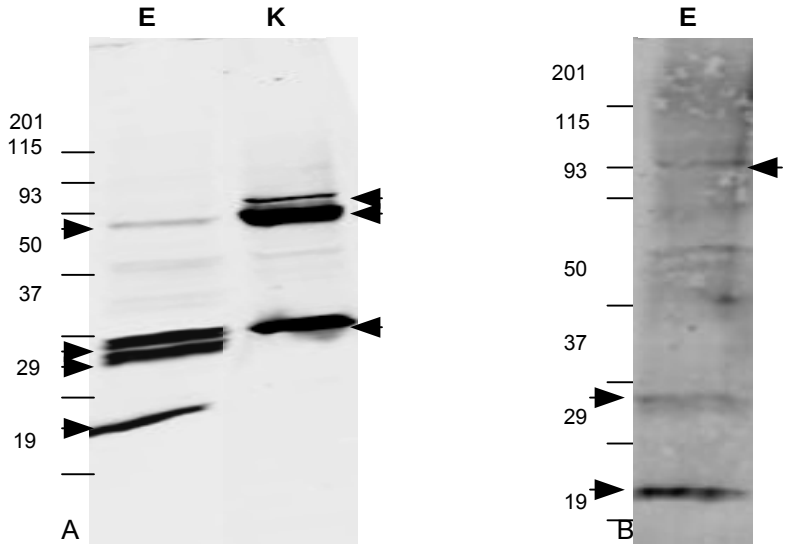

Figure 11. Western blots. Multiple bands were detected with KL-I from eye and kidney lysates (A). Dual bands were detected for ~35 and ~90 kDa. Additional bands of ~22 and ~33 kDa were also detected from eye lysates. KL-S only detected bands from eye lysates at ~22 and ~35 kDa (B). A possible band was detected for 115 kDa. E=eye; K=kidney. For more information, see blue binder in Haselton lab.

Klotho protein localized in RPE cells

Antibody staining revealed that the klotho protein was present in both the nucleus and cytoplasm of the RPE cell (Figure 12). Staining with KL-I produced a pattern of dark cytoplasm and bright nuclei that contained small punctate vesicles (Fig. 12, B). Nuclear membrane localization was also observed, seen as a bright ring around the nucleus. KL-S yielded the inverse of KL-I staining (Fig. 12, C). This pattern consisted of dark nuclei surrounded by granular, cytoplasmic staining. The protein appeared to be concentrated around the nucleus of the cell and diffused outward toward the cell membrane. Staining with the KL-B antibody produced a combination of the patterns seen with KL-I and KL-S (Fig. 12, D).

Dark nuclei containing faint, punctate vesicles were observed. The protein was concentrated around the nuclei and present throughout the cytoplasm. In confluent cells, the cell membrane was partly outlined by punctate granules. Cells stained with secondary antibody only showed no immunoreactivity (Fig. 12, A).

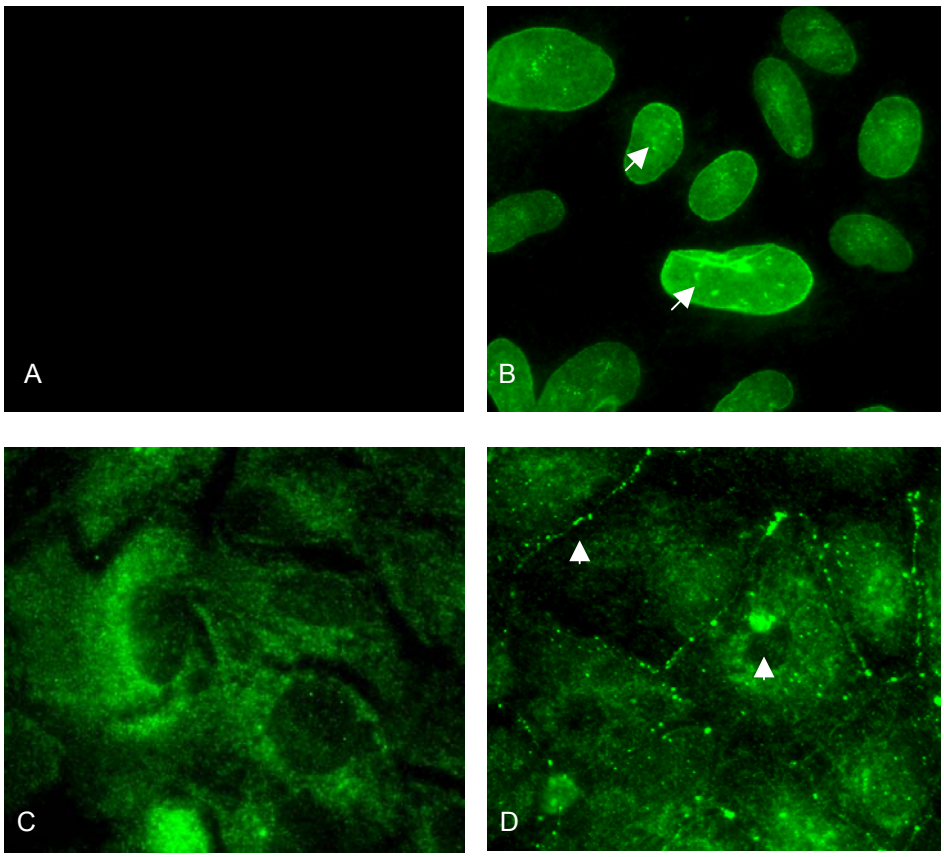

Figure 12**.** Immunofluorescent microscopy of ARPE cells. Control cells stained with 2° antibodies only (A). Cells stained with KL-I have dark cytoplasm and bright nuclei with punctate granules inside the nucleus (B, arrow) while KL-S staining gives a bright cytoplasm that surrounds a dark nucleus (C). KL-B staining gives a combination of KL-I and KL-S (D). Note the dark nuclei and punctate granules both in the cytoplasm, and on the cellular membrane (D, ▲).

Klotho staining of frozen sections

Staining of aged EFmKL46 and C57BL/6 retinal tissue produced inconclusive results (Figure 13). All neural layers of sections stained with only Alexa Fluor 488 were bright green (Fig 13, A). The cornea and choroid were also stained (data not shown). Immunostaining with KL-I gave results similar to the control staining seen in Figure 13, A (data not shown). Sections stained with KL-B and KL-S were also observed to have green neural layers, cornea, and choroid but fluoresced more brightly than controls (Fig 13, B-C). The outer limiting membrane and the membranes of cells located in the nuclear layers of the retina appeared to be more clearly distinguished with KL-B staining (Fig 13, B). Cell membranes were also more easily seen in sections stained with KL-S (Fig 13, C). Alexa Fluor 568 was used in an attempt to minimize background illumination caused by autofluorescence of the retinal tissue. C57BL/6 control retinas stained with only the secondary antibody produced results similar to those observed with only Alexa Fluor 488 used on EFmKL46 tissue (Fig 13, D). All retinal layers appeared red. These results were also observed for KL-I and KL-B staining (data not shown). KL-S staining allowed the visualization of individual cells in the nuclear layers of the retina (Fig 13, E). The protein appeared to be on the membrane of the cell.

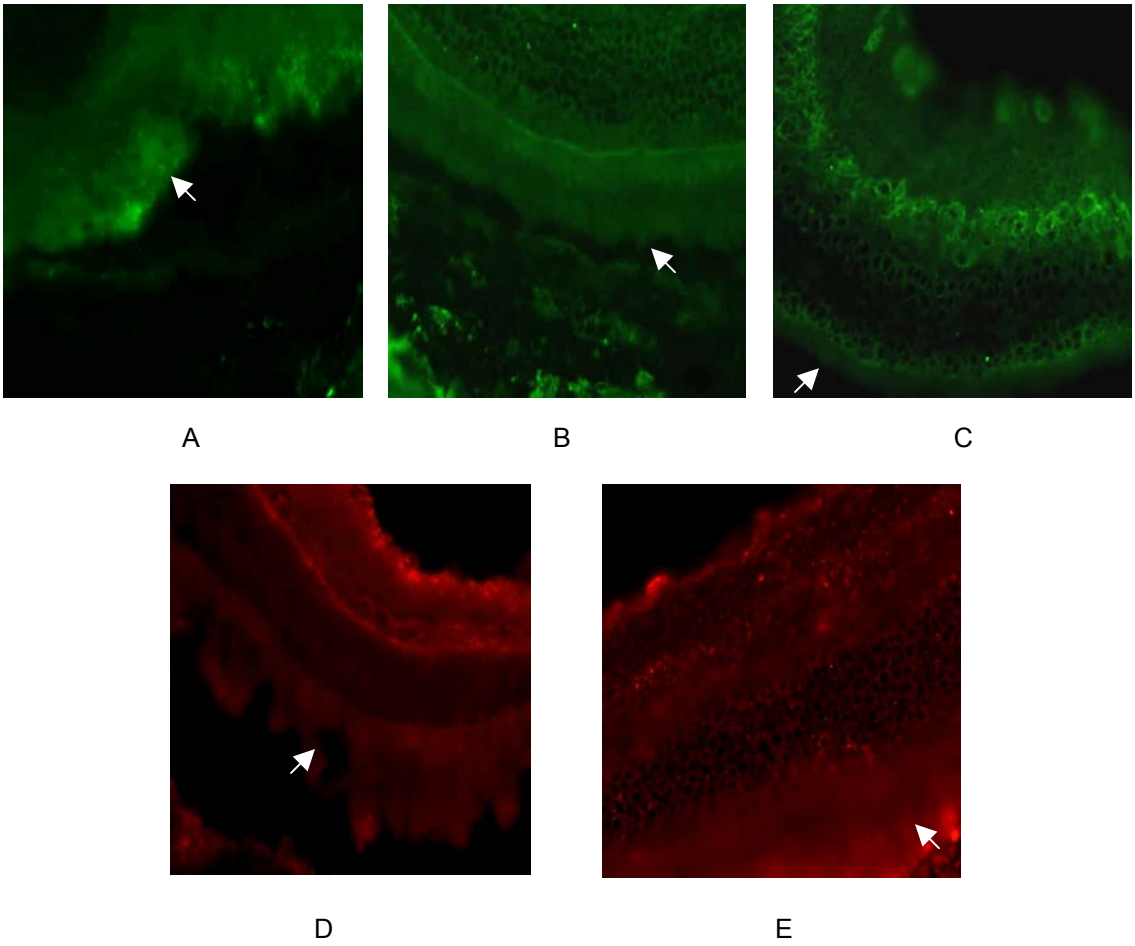

Figure 13**.** Immunofluorescent microscopy of frozen sections. Retinal tissue from aged EFmKL46 (A-C) and C57BL/6 (D-E) were stained with each klotho antibody. Sections stained with Alexa Fluor 488 only (A) were autofluorescent and all retinal layers appeared green. KL-B (B) and KL-S (C) staining gave a brighter signal and allowed for better visualization of the nuclear layers of the retina. KL-I antibody staining (data not shown) produced results similar to the control (A). C57BL/6 sections were stained with Alexa Fluor 568 in an attempt to minimize autofluorescence (D-E). KL-B and KL-I antibodies showed a staining pattern similar to the control stained with secondary only (D). KL-S allowed for better visualization of nuclear layers (E) but the image brightness was the same as in the control. Arrows indicate the photoreceptor layer.

Discussion

The presence of the klotho protein in the eye has not been previously studied. Western blotting and immunohistochemistry yielded promising results. Blots probed with the KL-I antibody specific for the intracellular portion of the klotho protein indicate 35 and 90 kDa bands in both the eyes and kidneys of

C57BL/6 mice. These numbers are far below the reported values of 120 and 135 kDa [21-24, 42]. One possible explanation is that the extracellular part of the protein has been shed at the cell surface and the antibody is detecting the remaining intracellular fragment. KM2119, an antibody specific for the second klotho repeat, has recognized a 60 kDa protein as well as a 130 kDa protein in mice and humans kidneys [21]. These scientists hypothesized the 60 kDa band was the result of cleavage of the membrane form. Part of the membrane protein had been cleaved, and the antibody was recognizing the remainder of the protein near the KL2 domain. The length of the protein fragment containing only the intracellular domain, in theory, would be shorter than a fragment that also contained the KL2 domain. As KL-I detected a 35 kDa band, this theory is plausible. The 90 kDa band detected in this work by KL-I in kidney lysate could be the result of cleavage of the extracellular domain at a different sight or the aggregation of two or more intracellular fragments. The more likely explanation is denaturation of the protein sample. However, it still remains to be determined if KL-I is actually detecting the klotho protein or the bands are a result of nonspecific binding. The lower band of 22 kDa detected in eye lysates with KL-I also remains to be explained.

KL-S, specific to the sequence of amino acids unique to the splice variant of the klotho protein, detected bands from eye lysates at ~ 22 and 35 kDa. These bands are roughly the same size as those detected with KL-I. An established antibody to the first klotho repeat (KM2076) has recognized a 130 kDa protein in wild type mice and human kidneys. This could be the full length of the klotho

protein or the splice variant as both include KL1. While the splice variant has only half the amino acids of the membrane-bound protein, the exact size of the splice variant has yet to be determined. KL-S did not detect the splice variant in the kidney lysate of mice. This may be due to the fact that the membrane form of klotho is expressed ten-fold that of the splice variant in all mouse tissue previously examined [24]. Therefore, the concentration of the splice variant was not great enough to be detected in the amount of kidney lysate used in this study.

Immunohistochemistry of RPE cells with the three klotho antibodies used in this study produced promising results. The antibody specific for the intracellular portion of the membrane protein, KL-I, localized this a.a. sequence in the nucleus of the cell. The extracellular portion of the membrane protein is broken off and secreted, and it is not known if the remainder of the protein remains attached to the cell membrane. This pattern of staining could indicate that the intracellular portion of the protein is released into the cytoplasm of the cell and is taken up by the nucleus. The punctate staining seen within the nucleus could indicate that the intracellular part of the protein is forming aggregates.

The secreted (or splice) variant of the protein is rarely mentioned in recent literature. Our antibody, KL-S, detected the splice variant form of the klotho protein in the cytoplasmic region of the cell. This form of the klotho protein appears to be more abundant in RPE cells than the membrane form detected with KL-I. This finding correlates with previous studies that determined the splice variant predominates over the membrane form in all tissue examined in humans,

such as the brain, prostate, and kidney [42]. As the retina can be thought of as an extension of brain, it is plausible that klotho is also abundant in the eye.

Immunostaining of RPE cells with the KL-B antibody produced a combination of KL-I and KL-S results. As KL-B is specific for the first extracellular repeat (KL1), the antibody appears to be detecting both the secreted splice variant and the membrane form. KL-B also detected the klotho protein in vesicles on the cell membrane. This may indicate that the extracellular domain of klotho is, in fact, being shed at the cell surface in RPE cells and supports the report that suggests that the secreted form of the membrane protein forms dimers and trimers and may group together to form aggregates [23].

The results from the frozen section staining can be interpreted in a variety of ways. The control staining with only a secondary antibody gave a fluorescent signal but visualization of the specific neural layers was not very clear. This could be attributed to autofluorescence of the retinal tissue, nonspecific binding or the secondary, or the inability to focus adequately due to the thickness of the tissue section. KL-B and KL-S appear to be located on the outer limiting membrane as well as the membranes of the cells located in the nuclear layers. This could indicate that klotho is, in fact, found on the cell surface of these cells in the retina especially since KL-B is specific for extracellular portion of the protein. The splice variant is also secreted at the cell surface and could account for KL-S staining.

As all the frozen retinal tissue fluoresced to some degree, it is difficult to determine how specific the antibodies are in the sections. As the retina fluoresces most around the 488 wavelength, Alexa Fluor 568 was used in

attempt to minimize the background effect, but with little success. Antibody and control staining gave very similar results. KL-S staining did allow for the visualization of the cell membranes in the nuclear layers, but KL-I and KL-B did not. This result is surprising as the membrane-bound fraction of klotho is more prominent in mouse tissue than the splice variant.

Appendix B

Table 1. Storage and use of klotho antibodies.

Klotho Antibodies (Rabbit)											
Peptide Sequence	Animal	Type	Fraction	Antibody labels	Amount (mL)	Concentration (mg/mL)	Storage (-20˚C)	Antibody tests		Antibody results	
								RPE	western	RPE	western
(C)SQLTKPISSLTKPYH-COOH A.A. #535-549 Klotho b	1b	SPL (KL-S)	KSCN	1bk	13.91	1.00	Original Tube	X	X	+++	++
			Glycine	1bg	5.93	1.00	Original Tube	X		+	
	2b	SPL (KL-S)	KSCN	2bk	13.20	0.45	Original Tube	X		++	
			Glycine	2bg	5.10	0.40	Original Tube	X		+	
(C)YYSKKGRRSYK-COOH A.A.#1002-1012 Klotho a	1c	INT (KL-I)	KSCN	1ck	10.98	1.00	Original Tube	X		++	
			Glycine	1cg	8.20	0.18	Original Tube	X		+	
	2c	INT (KL-I)	KSCN	2ck	14.91	1.00	0.5 mL aliquots	X	X	+++	+++
			Glycine	2cg	6.10	0.59	Original Tube	X		++	
(C)SGTTKRDDAKYMYY-NH_2 A.A. #420-433 Klotho a/b	1d	BOTH (KL-B)	KSCN	1dk	6.90	0.93	Original Tube	X		+	
			Glycine	1dg	6.00	0.87	Original Tube	X		+	
	2d	BOTH (KL-B)	KSCN	2dk	27.95	1.00	Original Tube	X	X	+++	-
			Glycine	2dg	6.00	0.67	Original Tube	X	X	+	+

SPL: splice variant, INT: intracellular, KSCN:, (+++): best for use, (++): adequate, (+): poor results, (-):no result. See pp. 44-46,54-56, 86-96 of lab book for additional details.

APPENDIX C

PERICYTE STAINING IN RETINAL WHOLE MOUNTS

Pericyte loss is one of the earliest cellular lesions seen in diabetic retinopathy. These cells surround capillary tubes in the retinal microcirculation and normally exist at a 1:1 ratio with endothelial cells. They are believed to serve a contractile function, help control the flow of blood through the capillaries, and possibly help maintain the blood retinal barrier. Pericyte dropout is usually observed in areas with nonperfused capillaries and microaneurysms. Pericyte loss may also account for a change in blood-retinal barrier permeability, one of the earliest signs of diabetic retinopathy [4].

Whole retinas were from aged EFmKL46 and C57BL/6 mice were removed from the eye, placed in 8-chambered slides, and washed with PBS-T (1% Triton X-100). PBS-T was then removed and the retinas were blocked overnight at 4°C in a solution of 1% Triton X-100, 5% horse serum, and 0.215% BSA in PBS. NG2 and biotinylated lection primary antibodies were added at concentration of 1:100 and 1:50 respectively and incubated overnight at 4°C. Retinas were washed with PBS three times for three minutes each. Streptavidin - Cy5, Alexa Fluor 555, and DAPI were then added to the samples at dilutions of 1:25, 1:1000, and 1:2000 respectively and incubated for 2 hours at room temperature. Retina were washed five times with PBS for 3 minutes each and covered with a coverslip. All slides were examined with an inverted fluorescence

microscope (Nikon Eclipse TE2000-U, Nikon, Inc., USA) with an EXFO X-Cite 120 Fluorescence Illumination System. Pictures were taken with a 3CCD Digital Camera (Hamamatsu C7780, Hamamatsu Photonics K.K., Hamamatsu City, Japan) and Image Pro software.

Aged C56BL/6 and EFmKL46 sections stained with NG2, biotinylated lectin, and DAPI gave similar results (Figure 14). NG2, an antibody specific for pericytes, gave poor staining results. The entire retina was red and pericytes could not be distinguished from other retinal tissue. Biotinylated lectin biotinylaed lectin stained retinal tissue as well as vessels red. However, the microvasculature could be distinguished. DAPI staining showed not only cells located along the walls of the microvessels as well as cells of the neural retina. Elongated cells lining the vessel wall were hypothesized to be pericytes due to their shape and location. C57BL/6 mice appeared to have more pericyte coverage along the length of the microvessels (Fig 14, A). EFmKL46 had less cellular localization along the vessel walls. Cells were also smaller and had a more circular morphology (Fig 14, B). Pericyte coverage was determined by visual inspection only. No quantative information could be gained from the images.

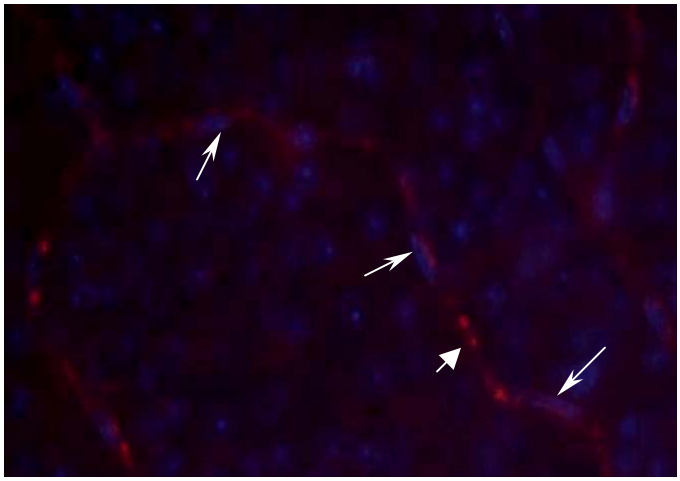

A

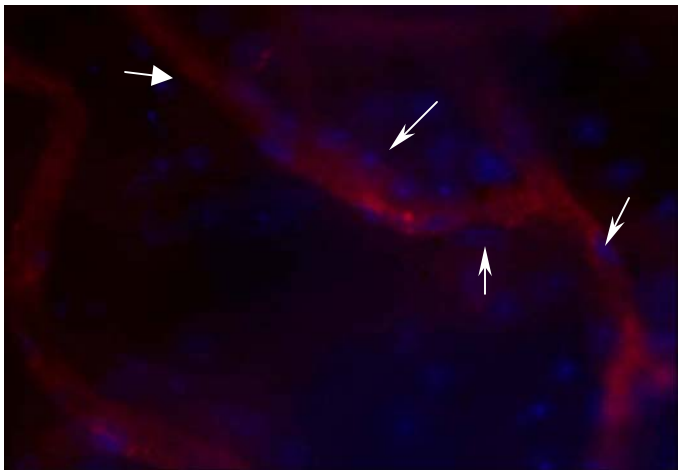

B

Figure 14. Pericyte staining of retinal whole mounts. Microvessels and cell nuclei were observed with immunostaining of aged C57BL/6 (A) and EFmKL46 (B) retina. C57BL6 had elongated nuclei that lined the outer edges of the blood vessels (A). The nuclei of other cells of the retina had a more rounded shape. EFmKL46 were also observed to have nuclei on the outer edge of the vessels. A few were elongated but most had a round morphology (B). Wide arrows indicate microvessels. Narrow arrows indicate possible pericytes.

Pericyte staining was very inconclusive. The NG2 antibody and its Alexa Fluor 568 secondary stained the entire retina red. Pericytes could not be definitively distinguished from the other retinal tissue. DAPI staining allowed for the localization of cell nuclei, but because the presence of pericytes could not be

confirmed, it is not known if the cells lining the microvessels are pericytes or another cell types. The elongated morphology of these vessel-lining cells is seen more in C57BL/6 than EFmKL46 retinas and pericyte loss is once of the landmarks of diabetic retinopathy. If these cells are, in fact, pericytes, this finding would help to further confirm that the vascular changes seen in aged EFmKL46 mice are the result of altered insulin signaling.

BIBLIOGRAPHY

1. Dowling, J.E., *The Retina: An Approachable Part of the Brain*. 1987, Cambridge: Belknap Press.

2. http://wbmo.mpimf-heidelberg.mpg.de/~teuler/Pics/retina1.htm. Accessed 28 June 2006.

3. Saltiel, A.R. and C.R. Kahn, *Insulin signalling and the regulation of glucose and lipid metabolism.* Nature, 2001. **414**(6865): p. 799-806.

4. Feman, S.S., ed. *Ocular Problems in Diabetes Mellitus*. 1992, Blackwell Scientific Publications: Boston.

5. http://arbl.cvmbs.colostate.edu/hbooks/pathphys/endocrine/pancreas/insulin_phys.html. Accessed 28 June 2006.

6. White, M.F., *The insulin signalling system and the IRS proteins.* Diabetologia, 1997. **40 Suppl 2**: p. S2-17.

7. Morris, J.Z., H.A. Tissenbaum, and G. Ruvkun, *A phosphatidylinositol-3-OH kinase family member regulating longevity and diapause in Caenorhabditis elegans.* Nature, 1996. **382**(6591): p. 536-9.

8. Tatar, M., et al., *A mutant Drosophila insulin receptor homolog that extends life-span and impairs neuroendocrine function.* Science, 2001. **292**(5514): p. 107-10.

9. Holzenberger, M., et al., *IGF-1 receptor regulates lifespan and resistance to oxidative stress in mice.* Nature, 2003. **421**(6919): p. 182-7.

10. Reiter, C.E. and T.W. Gardner, *Functions of insulin and insulin receptor signaling in retina: possible implications for diabetic retinopathy.* Prog Retin Eye Res, 2003. **22**(4): p. 545-62.

11. Reiter, C.E., et al., *Characterization of insulin signaling in rat retina in vivo and ex vivo.* Am J Physiol Endocrinol Metab, 2003. **285**(4): p. E763-74.

12. Fletcher, E.L., J.A. Phipps, and J.L. Wilkinson-Berka, *Dysfunction of retinal neurons and glia during diabetes.* Clin Exp Optom, 2005. **88**(3): p. 132-45.

13. L'Esperance, F.A., Jr., W.A. James, Jr., *Diabetic Retinopathy: Clinical Evaluation and Management*. 1981, St. Louis: Mosby.

14. Park, S.H., et al., *Apoptotic death of photoreceptors in the streptozotocin-induced diabetic rat retina.* Diabetologia, 2003. **46**(9): p. 1260-8.

15. Martin, P.M., et al., *Death of retinal neurons in streptozotocin-induced diabetic mice.* Invest Ophthalmol Vis Sci, 2004. **45**(9): p. 3330-6.

16. Aizu, Y., et al., *Degeneration of retinal neuronal processes and pigment epithelium in the early stage of the streptozotocin-diabetic rats.* Neuropathology, 2002. **22**(3): p. 161-70.

17. Barber, A.J., et al., *The Ins2Akita mouse as a model of early retinal complications in diabetes.* Invest Ophthalmol Vis Sci, 2005. **46**(6): p. 2210-8.

18. Yi, X., et al., *Insulin receptor substrate 2 is essential for maturation and survival of photoreceptor cells.* J Neurosci, 2005. **25**(5): p. 1240-8.

19. Barber, A.J., et al., *Neural apoptosis in the retina during experimental and human diabetes. Early onset and effect of insulin.* J Clin Invest, 1998. **102**(4): p. 783-91.

20. Kuro-o, M., et al., *Mutation of the mouse klotho gene leads to a syndrome resembling ageing.* Nature, 1997. **390**(6655): p. 45-51.

21. Kato, Y., et al., *Establishment of the anti-Klotho monoclonal antibodies and detection of Klotho protein in kidneys.* Biochem Biophys Res Commun, 2000. **267**(2): p. 597-602.

22. Nabeshima, Y., *Klotho: a fundamental regulator of aging.* Ageing Res Rev, 2002. **1**(4): p. 627-38.

23. Imura, A., et al., *Secreted Klotho protein in sera and CSF: implication for post-translational cleavage in release of Klotho protein from cell membrane.* FEBS Lett, 2004. **565**(1-3): p. 143-7.

24. Shiraki-Iida, T., et al., *Structure of the mouse klotho gene and its two transcripts encoding membrane and secreted protein.* FEBS Lett, 1998. **424**(1-2): p. 6-10.

25. Kurosu, H., et al., *Suppression of aging in mice by the hormone Klotho.* Science, 2005. **309**(5742): p. 1829-33.

26. Bartke, A., *Long-lived Klotho mice: new insights into the roles of IGF-1 and insulin in aging.* Trends Endocrinol Metab, 2006. **17**(2): p. 33-5.

27. Unger, R.H., *Klotho-induced insulin resistance: a blessing in disguise?* Nat Med, 2006. **12**(1): p. 56-7.

28. Ikushima, M., et al., *Anti-apoptotic and anti-senescence effects of Klotho on vascular endothelial cells.* Biochem Biophys Res Commun, 2006. **339**(3): p. 827-32.

29. Yamamoto, M., et al., *Regulation of Oxidative Stress by the Anti-aging Hormone Klotho.* J Biol Chem, 2005. **280**(45): p. 38029-34.

30. Yanoff, M., B. S. Fine, *Ocular Pathology, 5th ed.* 5th ed. 2002, St. Louis: Mosby.

31. Cho, N.C., et al., *Selective loss of S-cones in diabetic retinopathy.* Arch Ophthalmol, 2000. **118**(10): p. 1393-400.

32. Bloodworth, J.M., Jr., *Diabetic retinopathy.* Diabetes, 1962. **11**: p. 1-22.

33. Wolter, J.R., *Diabetic retinopathy.* Am J Ophthalmol, 1961. **51**: p. 1123-41.

34. Diaz, B., et al., *In vivo regulation of cell death by embryonic (pro)insulin and the insulin receptor during early retinal neurogenesis.* Development, 2000. **127**(8): p. 1641-9.

35. Bok, D., *New insights and new approaches toward the study of age-related macular degeneration.* Proc Natl Acad Sci U S A, 2002. **99**(23): p. 14619-21.

36. Russ, P.K., G.M. Gaylord, and F.R. Haselton, *Retinal vascular permeability determined by dual-tracer fluorescence angiography.* Ann Biomed Eng, 2001. **29**(8): p. 638-47.

37. Rice, D.S., et al., *Severe retinal degeneration associated with disruption of semaphorin 4A.* Invest Ophthalmol Vis Sci, 2004. **45**(8): p. 2767-77.

38. Voll, C.L. and R.N. Auer, *Insulin attenuates ischemic brain damage independent of its hypoglycemic effect.* J Cereb Blood Flow Metab, 1991. **11**(6): p. 1006-14.

39. Spraul, C.W., et al., *Effect of growth factors on bovine retinal pigment epithelial cell migration and proliferation.* Ophthalmic Res, 2004. **36**(3): p. 166-71.

40. Lev-Ran, A. and D.L. Hwang, *Epidermal growth factor and platelet-derived growth factor in blood in diabetes mellitus.* Acta Endocrinol (Copenh), 1990. **123**(3): p. 326-30.

41. Li, S.A., et al., *Immunohistochemical localization of Klotho protein in brain, kidney, and reproductive organs of mice.* Cell Struct Funct, 2004. **29**(4): p. 91-9.

42. Matsumura, Y., et al., *Identification of the human klotho gene and its two transcripts encoding membrane and secreted klotho protein.* Biochem Biophys Res Commun, 1998. **242**(3): p. 626-30.

43. Kerouz, N.J., et al., *Differential regulation of insulin receptor substrates-1 and -2 (IRS-1 and IRS-2) and phosphatidylinositol 3-kinase isoforms in liver and muscle of the obese diabetic (ob/ob) mouse.* J Clin Invest, 1997. **100**(12): p. 3164-72.